



STUDY OF HOMOGENEITY, POROSITY AND INTERNAL DEFECTS IN AERATED AND EPS AGGREGATE POLY BRICKS USING NEUTRON RADIOGRAPHY TECHNIQUE

¹Md. Khurshed Alam, ³Md. Sayeedur Rahman, ²Md. Mostafizur Rahman, ³S. M. Azaharul Islam

¹Institute of Nuclear Science and Technology, Bangladesh Atomic Energy Commission, AERE, Savar, Dhaka.
E- mail: alammk1964@yahoo.co.in

²Department of Chemical Engineering and Polymer Science, Shahjalal University of Science and Technology (SUST), Sylhet- 3114, Bangladesh.

Email: mostafizur.cep@gmail.com

³Department of Physics, Jahangirnagar University, Savar, Dhaka, Bangladesh.

Email: sayeed111ph@gmail.com

ABSTRACT

A powerful non-destructive testing (NDT) technique is adopted to study the internal defects and elemental distribution/homogeneity and porosity of aerated brick and EPS aggregate poly brick samples. In the present study the internal defects like homogeneity, porosity, elemental distribution, EPS aggregate and aerator distributor in the test samples have been observed by the measurement of gray value/optical density of the neutron radiographic images of these samples. From this measurement it is found that the neutron intensity/optical density variation with the pixel distance of the AOI of the NR images in both expanded polystyrene (EPS) aggregate poly brick and aerated brick samples comply almost same in nature with respect to the whole AOI but individually each AOI shows different nature from one AOI to another and it confirms that the elemental distribution within a AOI is almost homogeneous. Finally it was concluded that homogeneity, elemental distribution in the EPS aggregate poly brick sample is better than that of the aerated brick sample.

Keywords: neutron radiography; homogeneity; aerator and EPS aggregate poly

Council for Innovative Research

Peer Review Research Publishing System

Journal: JOURNAL OF ADVANCES IN PHYSICS

Vol.7, No.2

www.cirjap.com, japeditor@gmail.com



1. INTRODUCTION

Neutron radiography (NR) is a technique of making a picture of the internal details of an object by the selective absorption of a neutron beam by the object. NR uses the basic principles of radiography whereby a beam of radiation is modified by an object in its path and the emergent beam is recorded on a photo film (detector). NR is adopted for detection of internal defects such as, voids/ cavity, cracks, homogeneity [1], porosity etc. of industrial products/materials. In general, the radiography technique is a simple process of exposing some objects to an X-ray, gamma-ray, neutron beam and some other types of radiation and then attenuated out going beam from the object is passing through a special type of photographic film to form images of the objects on the radiographic film or detector. There are large numbers of brick kiln present in Bangladesh. This method is used for characterizing the internal structure, internal defects in automated machine made environmentally friendly brick and conventionally made brick samples [2-4], different ceramic samples [5], different tiles [6] and different building industries [7], internal defects in electronic components [8], water uptake and internal defects of jute reinforced polymer composite [9], water absorption behavior in biopol and jute reinforced biopol composite [10] etc.

In the NR mechanism the atoms of an object material scattered or absorbed the radiation and so the beam reaching the detector shows an intensity/gray value pattern representative of the internal structure of the object [11]. As a result NR images of the test samples gives the information of the internal structure of an object; can detect light elements, which have large neutron absorption cross-sections like hydrogen and boron; completely complementary to other NDT techniques such as X-ray or gamma ray radiography. The beam, which remains after passing through, enters a detector that registers the fraction of the initial radiation intensity that has been transmitted through each point/small pixel of the object. Any in-homogeneity in the object on an internal defect like voids, cracks, porosity, inclusion, corrosion etc. will show up as change in gray value/radiation intensity reaching the detector. The aim of the present work is to determination of the internal homogeneity, cracks, voids, elemental distribution of EPS aggregate and creation of porosity in the EPS aggregate poly brick and creation of aerator inside aerated brick samples.

1. EXPERIMENTAL FACILITY

A beam of thermal neutron having energy 0.025eV is used in this experiment. This is the most suitable energy of neutron for NR experiment. In the present study a well established NR facility [12-13] of BTRR (BAEC Triga Research Reactor) is used. The NR facility consists of bismuth filter, cylindrical divergent collimator, lead shutter, beam stopper, sample and camera holder table, beam catcher and a biological shielding house which is made of special concrete containing cement, heavy sand (magnetite, ilmenite and ordinary sand) and stone chips in the ratio 1:3: 3, paraffin wax and boric acid in 3:1 ratio by weight for neutron shielding.

3. EXPERIMENTAL PROCEDURE

3.1. Sample collection and preparation

Portland cement, aluminum powder, sand were collected from local market. Portland cement of ASTM type CEM II is used to prepare aerated brick sample. The expanded polystyrene (EPS) collected from local market is used in making EPS aggregate poly block sample.

3.1.1. Portland cement

The chemical composition and some other characteristics (in weight percent) of the Portland cement are as follows: CaO- 63.58%, SiO₂- 20.44%, Al₂O₃- 5.34%, Fe₂O₃- 4.0%, Loss on ignition-1.10%, Insoluble residue- 0.07% and Moisture content- 0.5%. The standard test-properties of the Portland cement used as binder in the experiment are evaluated following the ASTM standard methods. It is found that initial setting time of the cement is 2 hr, final setting time 3 hr, fineness 0.068% and average compressive strength 19 MPa. For creation of large number of air gap/aerator in the brick carbonic acid gas (aerated water) was used.

3.1.2. Sand

Particle size of the fine aggregates is in the range of $0.15 \leq x \leq 4.75$ mm, about 50% of the fine aggregates are with sizes $4.75 > x \geq 0.9$ mm, the specific gravity, fineness of modulus is 2.6 and 2.5 0, respectively and the maximum EPS aggregates size of 4.75 mm were used.

Both types of bricks are made using the traditional method known as 'hand-moulding' and dried in air (usually in the sun/environment) until they were strong enough for use and light weight bricks (also called lightweight blocks). Both types of brick are produced in numerous types, materials, and sizes which vary with region and time period, and are produced in bulk quantities.

Finally both the samples are polished manually by using series paper, cement block, diamond cutter and was dried at day light/dryer machine at 65°C until to get the constant weight. The actual size, shape and weight of each final sample are $23.464 \times 11.026 \times 6.416$ cm³, rectangular in shape and weight 3305.00 gm, respectively.



3.2. Loading converter foil and film in the NR-cassette

A thin converter (gadolinium metal foil of 25 μm thickness) was placed at close contact with the emulsion surface of the X-ray industrial film. The loading of the X-ray industrial film (Agfa structurix D₄DW) into the NR cassette (18 cm x 24 cm) is a simple procedure [14] which requires a darkroom.

3.3. Placing of sample and the NR-cassette in the experimental facility

The sample is placed in close contact with the NR cassette on the sample holder table. The NR cassette is placed on the cassette holder table. Both of NR cassette and sample are placed in front of the neutron beam.

3.4. Determination of sample exposure time

Exposure means passing of neutron beam through a sample and holding it onto a special film (X-ray industrial film) in order to create a latent internal image of an object in the emulsion layers of that film. Exposure time differs for different samples, depending on the intensity of the neutron beam, neutron cross-section, density and thickness of the sample. The optimum exposure time of the dry sample was determined by taking a series of neutron radiographs with different exposure time, while the reactor was operated at constant power 2.4 MW. In the present experiment the optimum exposure time is found 08 minutes for each sample. The samples were then irradiated for that optimum exposure time to obtain good neutron radiographic images (Fig. 1 – Fig.3) of each sample one by one.

3.5. Obtained radiographic images

To obtain the neutron radiographic images of these samples the following procedures are completed.

3.5.1. Irradiation: After putting the sample on the sample holder table the neutron beam was disclosed by removing the wooden plug, lead plug and beam stopper from the front side of the collimator.

3.5.2. Developing: Developing is an image processing technique by which the latent image (recorded during the exposure of the material) is converted into a metallic silver image [15]. Developing process is completed at 20°-22°C for 07 minutes.

3.5.3. Fixing: The fixation solution will dissolve the unexposed silver-halide crystals leaving only the silver grains in the gelatin of the exposed film. The fixing is completed with in a 05 minutes and control the fixture temperature at 20°-22°C.

3.5.4. Washing: In between developing and fixing the radiographic film, it is necessary to wash for 1 minute at flowing tap water.

3.5.5. Final washing: The silver compound was formed during the fixing stage must be removed, since they can affect the silver image at the latter stage. For this reason the film must be washed thoroughly in flowing tap water for 15 minutes after completion of developing and fixing process of the exposed film.

3.5.6. Drying: After final washing, the films were dried by clipping in a hanger at fresh air/or in a drying cabinet.

4. MATHEMATICAL FORMULATION

Homogeneity/or internal defects e.g. voids, cracks, porosity, aerator and elemental distribution of EPS aggregate will show up as a change in gray value/neutron intensity reaching the detector. The intensity/gray value variation obeys the following general attenuation law [16], applicable for X-rays, gamma rays or neutrons:

$$I = I_0 e^{-\mu x} \quad (1)$$

Where,

I_0 = intensity of the incident neutron beam,

I = intensity of the emergent beam from the object,

μ = neutron attenuation coefficient,

x = thickness of the test object.

The attenuated neutrons beam enters the detector that resists the fraction of initial radiation intensity that has been transmitted by each point of the object and is then recorded by the radiographic film i.e. image detector.

4.1. Optical density measurement

The neutron intensity before reaching the aerated and aggregate poly brick sample (object) is different from the intensity of the neutron after passing through the samples. The relationship between these two intensities is expressed through the equation (1). On the other side of the film, a light sensor (photocell) converts the penetrated light into an electrical signal. A special circuit performs a logarithmic conversion on the signal and displays the results in density units.



The primary use of densitometers in a clinical facility is to monitor the performance of film processors. Actually, optical density is the darkness or opaqueness of a transparency film and is produced by film exposure and chemical processing. An image contains areas with different densities that are viewed as various shades of gray.

4.2. Gray value

The visual appearance of an image is generally characterized by two properties such as brightness and contrast. Brightness refers to the overall intensity level and is therefore influenced by the individual gray-level (intensity) values of all the pixels within an image. Since a bright image (or sub image) has more pixel gray-level values closer to the higher end of the intensity scale, it is likely to have a higher average intensity value. Contrast in an image is indicated by the ability of the observer to distinguish separate neighboring parts within an image. This ability to see small details around an individual pixel and larger variations within a neighborhood is provided by the spatial intensity variations of adjacent pixels, between two neighboring sub images or within the entire image. Thus, an image may be bright (due to, for example, overexposure or too much illumination) with poor contrast if the individual target objects in the image have optical characteristics similar to the background. At the other end of the scale, a dark image may have high contrast if the background is significantly different from the individual objects within the image, or if separate areas within the image have very different reflectance properties. For a captured image with maximum and minimum gray-level values g_{\max} and g_{\min} , and using the sinusoidal image intensity. Image contrast modulation and mean brightness are given by the following equation:

$$\text{Contrast modulation} = [g_{\max} - g_{\min}] / [g_{\max} + g_{\min}] \quad (2)$$

Although the intensity distribution within any real-life image is unlikely to be purely sinusoidal, these definitions provide a basis for comparison. For example, an image that contains pixels with brightness values spread over the entire intensity scale is likely to have better contrast than the image with pixel gray-level values located within a narrow range. The relationship between the intensity spread at the pixel level and the overall appearance of an image provides the basis for image enhancement by gray-level transformation. The terms gray value and intensity are used synonymously to describe pixel brightness.

4. RESULTS AND DISCUSSION

The specific relationship between the shades of gray or density and exposure depends on the characteristics of the film emulsion and the processing conditions. The quality of each brick sample depends on the proper elemental distribution, porosity, hardness, water penetration/absorption behavior etc. Figure 4 (a-b) and Fig. 5 (a-b) show the gray value/neutron intensity variation of different area of interest (AOI) with the pixel distance of the EPS aggregate brick sample and the aerated brick sample, respectively. The gray value of interested AOI of size (30 × 1148) pixel at different levels (level 1 to level 6) have been measured by drawing horizontal line profile of this AOI at each level on the radiographic image plane of each object. The gray value/intensity of each level at same AOI is almost identical with respect to the whole AOI in both the cases. But the variation is observed when compare from one level to another level. At the same time section of size 300 × 300 pixels of radiographic images (Fig. 1a) of aerated bricks and EPS aggregate poly bricks image (Fig. 1b) were investigated to measure the sample's internal in homogeneity, elemental distribution, cracks, porosity, creation of aerator and distribution of EPS aggregate. In case of aerated brick sample Fig. 1(a) and Fig. 2 show that (a) there is no crack is present, (b) at few places the creation of aerator is large number and at some places its number is poor (c) creation of aerator is not homogeneous all over the manufactured aerated brick sample. It also shows that different shapes such as dumbly, circular, oval shape aerator water was created in the sample. From this investigation it is concluded that the large number and shape of porosity/aerated water is created inside the aerated brick sample. The size of that aerator i.e., the created porosity is about 1mm-3mm. On the other hand in case of EPS aggregate brick (Fig. 1b and Fig. 3) it show that different shape of the EPS aggregate is mixed in the aggregate brick sample and observed that size of 1mm-2mm porosity is created in the poly brick, the distribution of EPS aggregate is almost homogeneous. No cracks are observed and small number of porosity is exists in the sample. The EPS aggregate and aerator appear black (Fig. 2 and Fig. 3) with a random distribution of size.

The neutron transmission profile graph (Fig. 4) show that transmission of neutron through the different levels of the same sample is almost same with respect to the whole area of the radiographic image of the EPS aggregate poly brick sample. One may conclude that the contents of EPS aggregate in each level/AOI is slightly different. It also concludes that the EPS aggregate are almost uniformly distributed in the sample. This type of bricks is used for building, block paving and pavement. In the USA, brick pavement was found incapable of withstanding heavy traffic, but it is coming back into use as a method of traffic calming or as a decorative surface in pedestrian precincts. For example, in the early 1900s, most of the streets in the city of Grand Rapids, Michigan were paved with brick. Today, there are only about 20 blocks of brick paved streets remaining (totalling less than 0.5 percent of all the streets in the city limits) [17].

In Northwest Europe, bricks have been used in construction for centuries. Until recently, almost all houses were built almost entirely from bricks. Although many houses are now built using a mixture of concrete block and other materials, many houses are skinned with a layer of bricks on the outside for aesthetic appeal. The experimental results of Murali et al emphasized that increasing the number of the steel mesh layers in the ferrocement composites increases energy at first cracking, energy at up to failure, and energy absorption properties [18].

The contents of the EPS aggregate brick sample is uniformly mixed and simultaneously, it is confirm that little bit pores are exist at the less homogeneous part of the sample. The measurements of optical density values it shows that, at one end the optical density is higher than the other end. Higher optical density ends having little bit greater pores and greater in-

homogeneity than the other end. Optical density is the darkness or opaqueness of a transparency film and is produced by film exposure and chemical processing. Two most basic categories of brick are available in the world. They are fired and non-fired brick. Fired brick are one of the longest lasting and strongest building materials sometimes referred to as artificial stone and have been used since circa 5000 BC. In our case the produced brick is non-fired. In near future this result will be helpful to compare the quality between fired and non-fired brick. The use of these brick has largely remained restricted to small to medium sized buildings, as steel and concrete remain superior materials for high-rise construction. It has great advantages is to minimise the building weight $1/10^{\text{th}}$ (if we use only different interior partition/wall) of the building weight made by conventional brick. The use of EPS as aggregate and cement replacement has been successfully applied to the production of a more eco-friendly, lightweight concrete brick [19]. Moreover, the moisture migration and absorption results indicate that the EPS concrete containing bigger size and higher volumes of EPS aggregate show higher moisture migration and absorption [20]. The neutron transmission profile graph (Fig. 4) shows that transmission of neutron through the different levels of the same sample is almost same with respect to the whole area of the radiographic image of the EPS aggregate poly brick.

The aerated brick can be used for commercial, industrial and residential construction. The resultant building material, comprising millions of tiny air pores, non-toxic, reusable, renewable and recyclable. It was developed in 1924 by a Swedish architect, who was looking for an alternate building material with properties similar to that of wood – good thermal insulation, solid structure and easy to work with – but without the disadvantage of combustibility, decay and termite damage. It is non-polluting manufacturing process, does not exude gases such as (SO_x, NO_x etc), 3-4 times lighter than traditional bricks, therefore, it is easier and cheaper to transport, reduces overall dead load of a building, tiny air pores (1mm-3mm) and thermal mass of blocks provide excellent thermal insulation, thus reducing heating and air conditioning costs of a building, non-combustible and fire resistant up to 1600° C, superior sound absorption qualities due to porous structure of blocks, blocking out all major sounds and disturbances. It is also ideal for schools, hospitals, hotels, offices, multi-family housing and other structures that require acoustic insulation, blocks can be easily cut, drilled, nailed, available in custom sizes, lightweight blocks reduce mass of a structure, thus decreasing the impact of an earthquake on a building, non-combustible nature provides an advantage against fires, results in smooth walls with perfect contact between different elements, reduces cement and steel usage, reduces operating cost by 30% to 40%, reduces overall construction cost by 2.5% as it requires less jointing, wall painting and plastering last longer, reduces construction time by 20%, different sizes of blocks help reduce the number of joints in wall masonry, lighter blocks make construction easier and faster, easy to install [21].

6. CONCLUSION

The investigations concluded that EPS aggregate poly brick sample is better than that of the aerated brick sample. It is also mentioned that this technique is very useful to detect the internal defects in the various types of clay and with out clay brick sample. Aerated bricks and poly blocks are light weight building materials can be used as building materials in external wall. EPS based waste packaging material can provide light weight properties to the modified concrete, which is significant for floating structure and where light weight material is recommended.

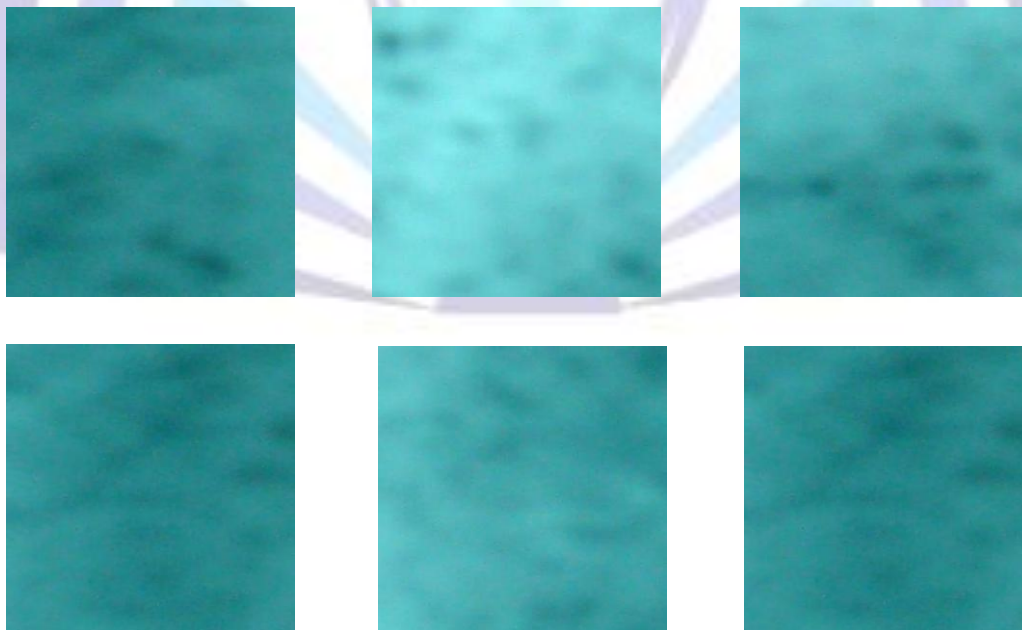


Fig. 1 (a) Section images of aerated brick

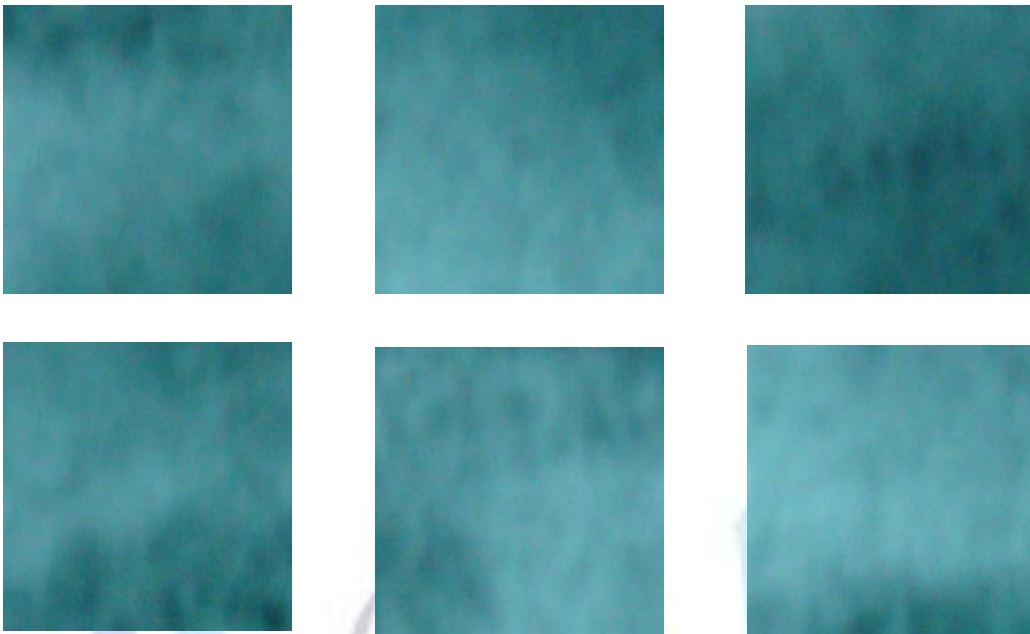


Fig. 1 (b) Section images of EPS aggregate poly brick

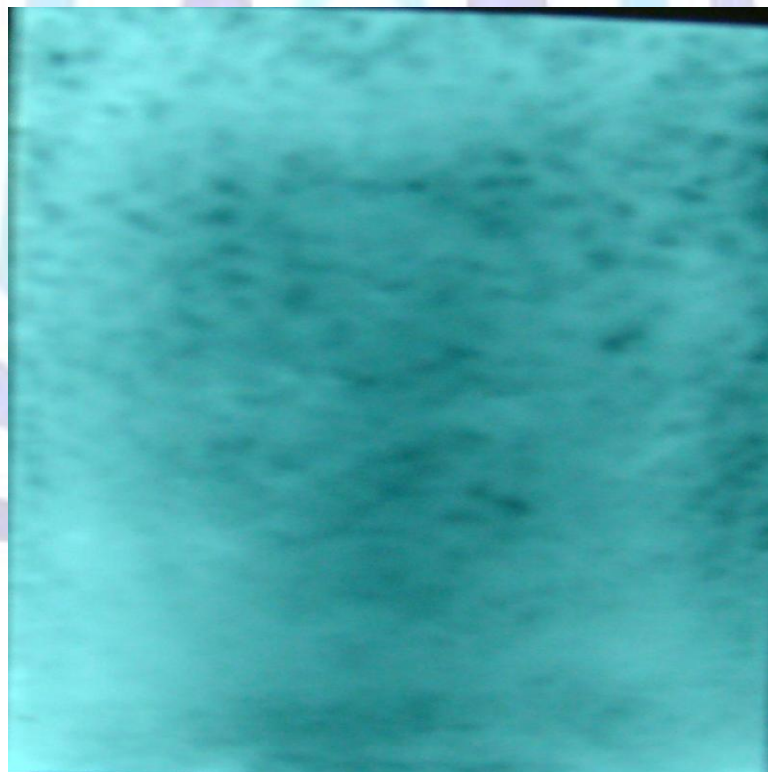


Fig. 2 Neutron radiographic image of Aerated brick (size 1153 X 1379 pixel)

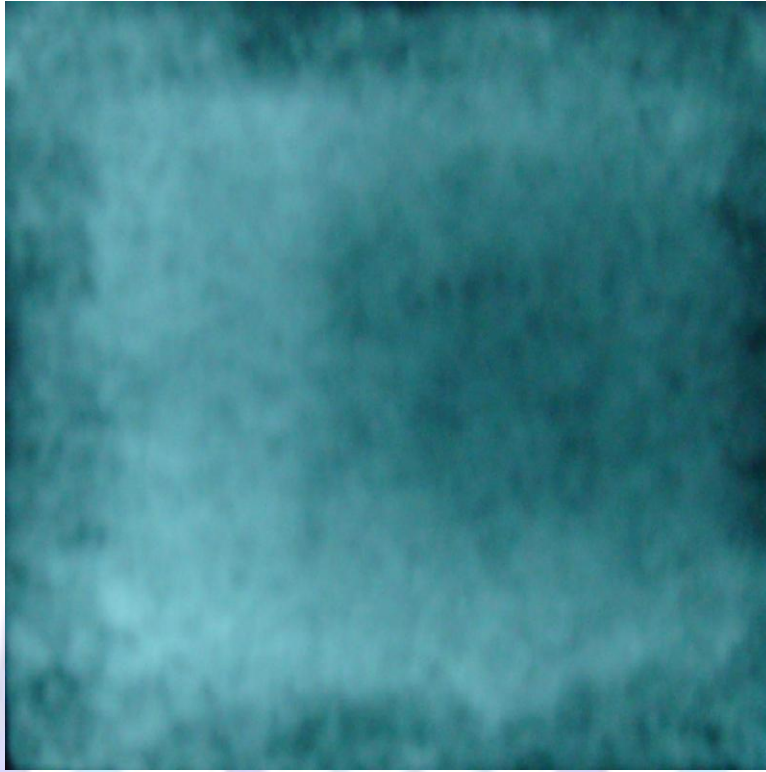


Fig. 3 Neutron radiographic image of EPS Aggregate poly brick (size 1153 X 1175 pixel)



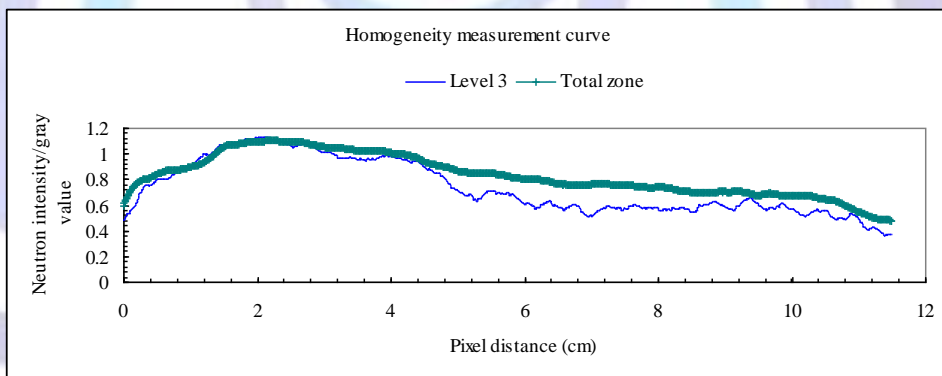
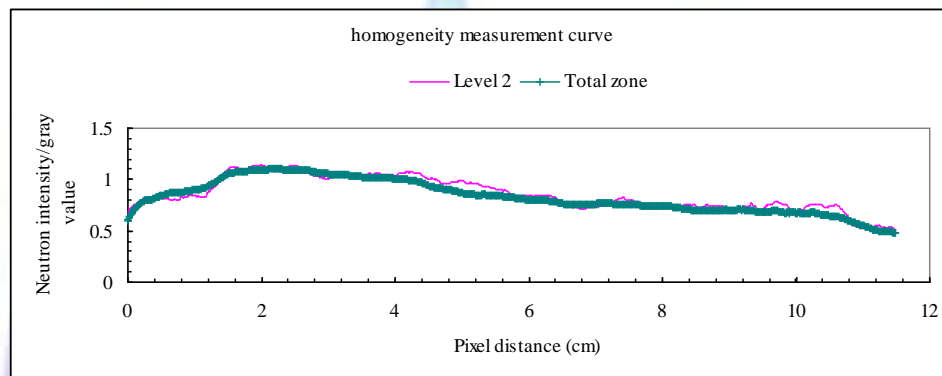
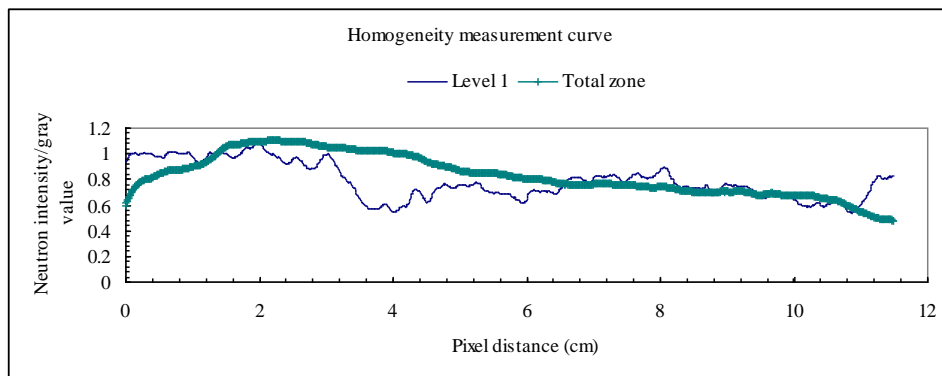


Fig.4a Pixel distance vs. neutron transmission at different levels of EPS aggregate poly brick

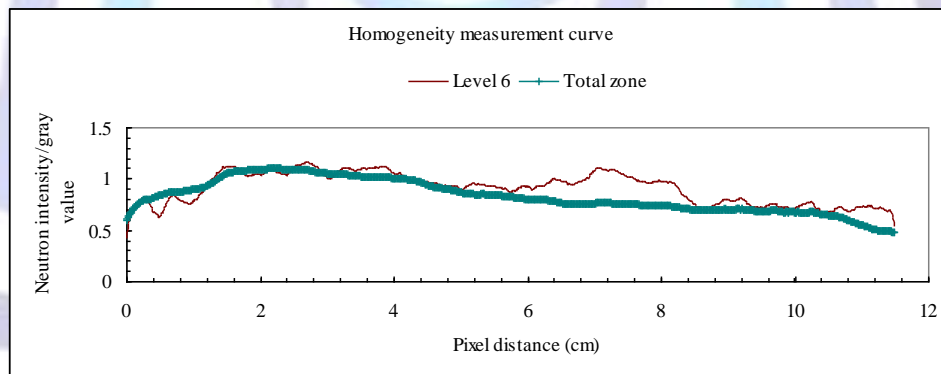
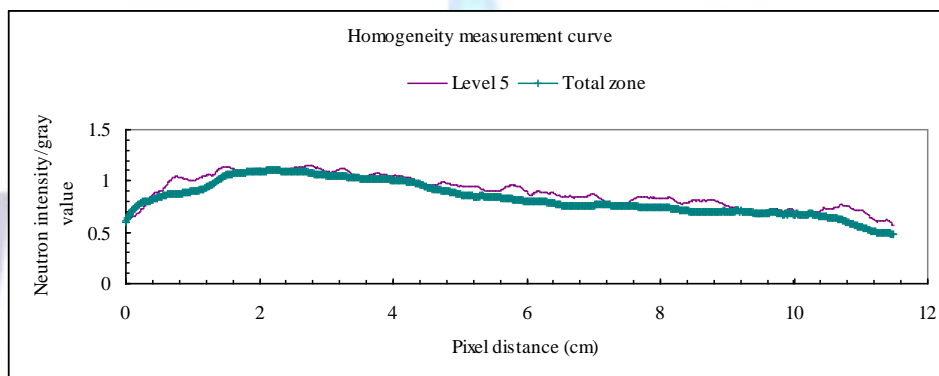
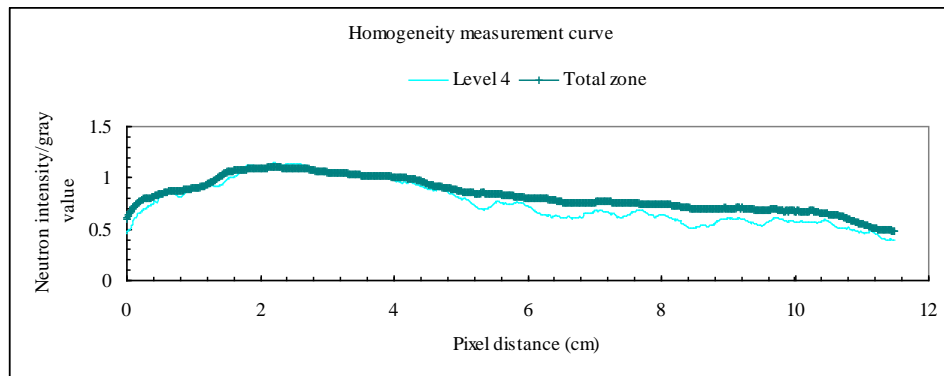


Fig.4b Pixel distance vs. neutron transmission at different levels of EPS aggregate poly brick

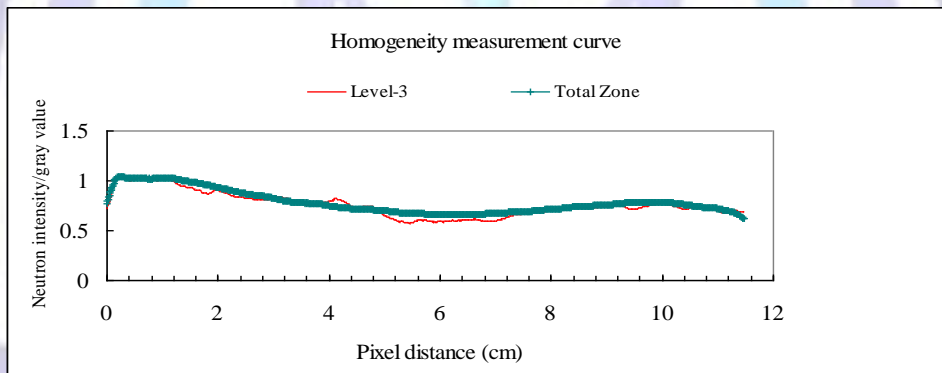
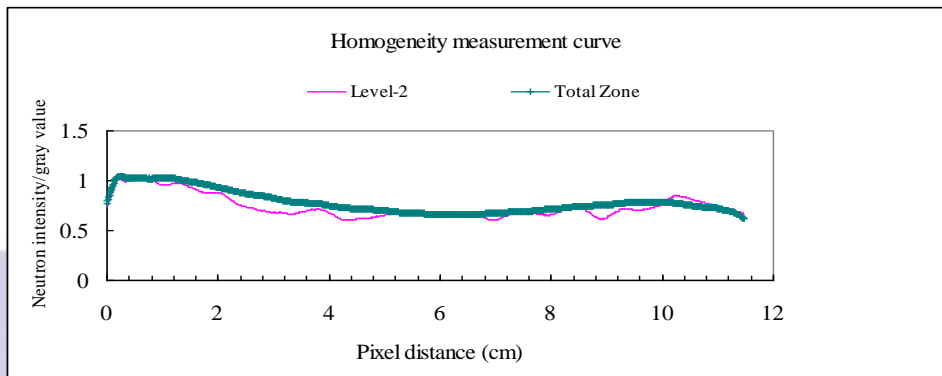
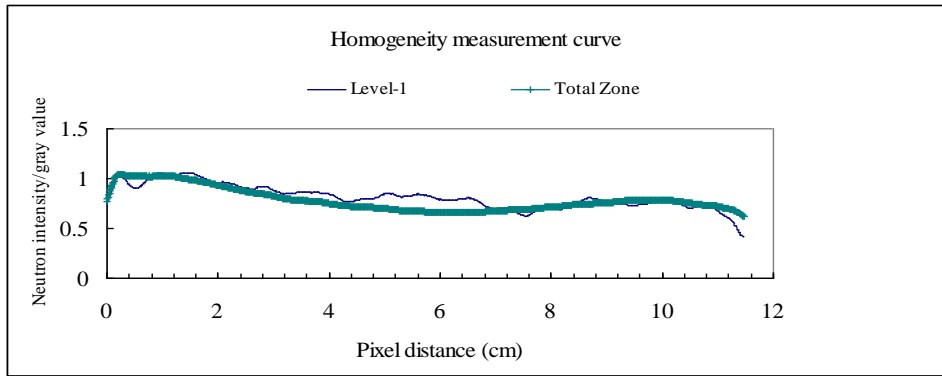


Fig.5a Pixel distance vs. neutron transmission at different levels of aerated brick

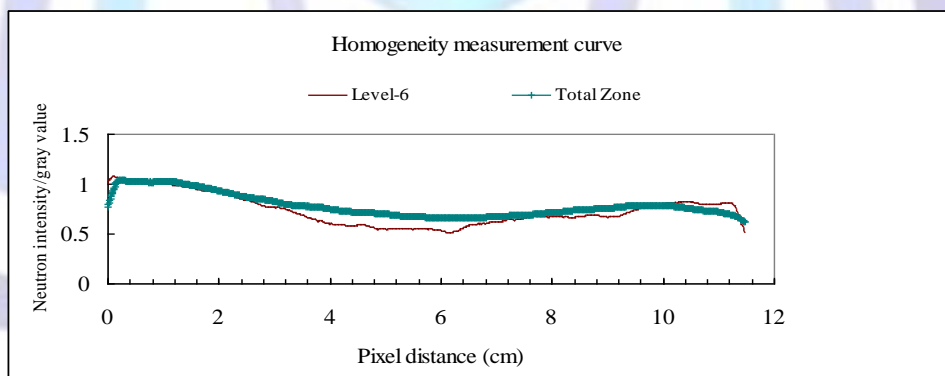
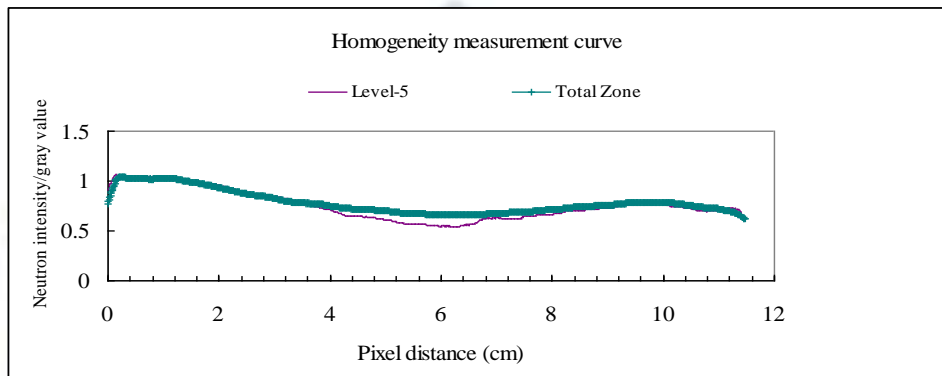
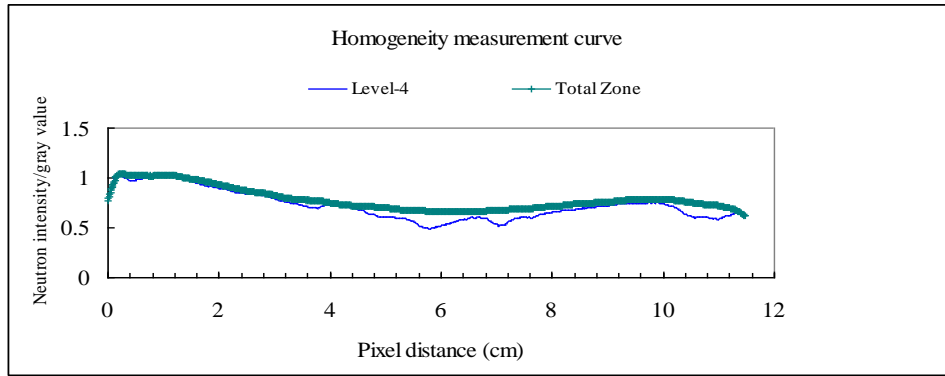


Fig.5 b Pixel distance vs. neutron transmission at different levels of aerated brick

FIGURE CAPTIONS

Fig. 1 Section image of the neutron radiographic image of (a) aerated brick (b) EPS poly brick.

Fig. 2 Neutron radiographic image of aerated brick sample.

Fig. 3 Neutron radiographic image of EPS aggregate poly brick sample.

Fig. 4 Pixel distance vs. neutron transmission at different levels of EPS aggregate poly brick.

Fig. 5 Pixel distance vs. neutron transmission at different levels of aerated brick.



REFERENCES

- [1] Alam, M. K., and Khan, M. A. 2006. Study of water absorption and internal defects in jute reinforced biopol composite using digital neutron radiography technique. *Journal of Bangladesh Academy of Sciences* 30, 29.
- [2] Alam, M. K., Islam, R., Saha, S., Islam N., and Islam, S. A. 2013. Quality study of automated machine made environmentally friendly brick (kab) sample using film neutron radiography technique. *Journal of Building Construction and Planning Research*, 1 (4), 141-152.
- [3] Alam, M. K., Islam, M. R., Saha S., Islam M.N., and Islam S. M. A. Quality study of hand made brick-dk using neutron radiography technique. 2013. *Bangladesh Journal of the Scientific and Industrial Research*, 48 (4), 237-246.
- [4] Alam, M. K., Islam, M. R., Saha, S., Islam, M.N., and Islam, S. M. A. 2014. Internal defects and water absorption behavior of environmentally friendly brick-MAB using film neutron radiography technique. *Journal of Bangladesh Academy of Sciences*, 38 (1), 1-6.
- [5] Alam, M. K. 2005. Comparative study of internal defects in ceramic products using CCD-camera based digital neutron radiography detector. *Bangladesh J. Sci. Ind. Res.*, 40(3-4), 169.
- [6] Alam, M. K., Islam, M. N., and Zaman, M. A. 2007. Study of internal defects and water absorption behavior of single layer Italian tiles using neutron radiography facility of 3 MW TRIGA MARK II research reactor. *Journal of Bangladesh Academy of Sci.*, 31(2), 213.
- [7] Islam, M. N., Alam, M. K., Zaman, M. A., Ahsan, M. H., and Molla, N. I. 2000. Application of neutron radiography to building industries. *Indian Journal of Pure and Applied Phys.*, 38, 348.
- [8] Mia, S., Rahman, M. H., Saha, S., Khan, M. A. T., Islam, M. A., Islam, M. N., Alam, M. K., and Ahsan, M. H. 2013. Study of the internal structure of electronic components RAM DDR-2 and motherboard of nokia-3120 by using neutron radiography technique. *International Journal of Modern Engineering Research (IJMER)*, 3 (60), 3429-3432.
- [9] Alam, M. K., Khan, M. A., Lehmann, E. H., and Vontobel, P. 2007. Study of water uptake and internal defects of jute reinforced polymer composites using digital neutron radiography technique. *Journal of Applied Polymer Science*, 105, 1958.
- [10] Alam, M. K., Khan, M. A., and Lehmann, E. H. 2006. Comparative study of water absorption behavior in Biopol[®] and jute-reinforced biopol[®] composite using neutron radiography technique. *Journal of Reinforced Plastics and Composites*, 25(11), 1179.
- [11] Hardt, P. Von der, and Rotterger, H. 1981. *Neutron radiography hand book*. D. Reidel Publishing Company, Dordrecht, Holland.
- [12] Ahsan, M. H., Islam, M. N., and Alam, M. K. 1995. Proc. of the 2nd international topical meeting on neutron radiography system design and characterization. Rikkyo University, Japan, Nov. 12-18., 30.
- [13] Islam, M. N., Rahman, M. M., Ahsan, M. H., Mollah, A. S., Ahsan, M. M., and Zaman, M. A. 1995. *Jahangirnagar University Journal of Sci.*, 19, 181.
- [14] Bouma, A. H. 1969. *Methods for the study of sedimentary structures*. A text book, Publisher by John Wiley and Sons and the author Arnold Bouma, New York, pp. 140.
- [15] Bjelkhagen, H. I. 1993. *Silver-halide recording materials*. Springer Verlag, pp. 128-151.
- [16] Norris, P. M., Brenizer, J. S., Paine, D. A., and Bostain, D. A. 1996. Measurements of water deposition in aerogel by neutron radiography. *Proc. 5th World Conf. on Neutron Radiography*, Berlin, Germany, June 17-20. pp.602.
- [17] http://en.wikipedia.org/wiki/Brick#cite_note-21.
- [18] Murali, G., Arun, E., Arun, A. P., Infant, R. R., and Prasanth, T. A. 2014. Experimental investigation of reinforced ferrocement concrete plates under impact load. 2014. *international journal of latest research in engineering and computing (IJLREC)*, 2 (1), 01-04, web site: www.ijlrec.com.
- [19] Ling, I. H., and Teo, D. C. L. 2013. EPS RHA Concrete bricks – a new building material. *Jordan Journal of Civil Engineering*, 4, 361.
- [20] Babu, D. S., Babu, K. G., and Tiong-Huan, W. 2006. Effect of polystyrene aggregate size on strength and moisture migration characteristics of lightweight concrete, *Journal of the Cement and Concrete Composites*, 28 (6), 520–527.
- [21] <http://www.biltechindia.com/biltech-ace-aac-benefits-advantages.asp?links=b3>.